

# 1 Introduction to the French GEOTRACES North Atlantic Transect

## 2 (GA01): GEOVIDE cruise

3

4 Sarthou Géraldine <sup>1</sup>, Lherminer Pascale <sup>2</sup>, Achterberg Eric P. <sup>3</sup>, Alonso-Pérez Fernando <sup>4</sup>,  
5 Bucciarelli Eva <sup>1</sup>, Boutorh Julia <sup>1</sup>, Bouvier Vincent <sup>5</sup>, Boyle Edward A. <sup>6</sup>, Branellec Pierre <sup>2</sup>,  
6 Carracedo Lidia I. <sup>4</sup>, Casacuberta Nuria <sup>7</sup>, Castrillejo Maxi <sup>7,8</sup>, Cheize Marie <sup>1,9</sup>, Contreira Pereira  
7 Leonardo <sup>10</sup>, Cossa Daniel <sup>11</sup>, Daniault Nathalie <sup>2</sup>, De Saint-Léger Emmanuel <sup>12</sup>, Dehairs Frank <sup>13</sup>,  
8 Deng Feifei <sup>14</sup>, Desprez de Gésincourt Floriane <sup>1,2</sup>, Devesa Jérémy <sup>1</sup>, Foliot Lorna <sup>15</sup>, Fonseca-  
9 Batista Debany <sup>13,16</sup>, Gallinari Morgane <sup>1</sup>, García-Ibáñez Maribel I. <sup>4,17</sup>, Gourain Arthur <sup>1,18</sup>,  
10 Grossteffan Emilie <sup>19</sup>, Hamon Michel <sup>2</sup>, Heimbürger Lars Eric <sup>20</sup>, Henderson Gideon M. <sup>14</sup>,  
11 Jeandel Catherine <sup>5</sup>, Kermabon Catherine <sup>2</sup>, Lacan François <sup>5</sup>, Le Bot Philippe <sup>2</sup>, Le Goff Manon  
12 <sup>1</sup>, Le Roy Emilie <sup>5</sup>, Lefèbvre Alison <sup>2</sup>, Leizour Stéphane <sup>2</sup>, Lemaitre Nolwenn <sup>1,13,21</sup>, Masqué Pere  
13 <sup>8,22,23</sup>, Ménage Olivier <sup>2</sup>, Menzel Barraqueta Jan-Lukas <sup>3,24</sup>, Mercier Herlé <sup>2</sup>, Perault Fabien <sup>12</sup>,  
14 Pérez Fiz F. <sup>4</sup>, Planquette Hélène F. <sup>1</sup>, Planchon Frédéric <sup>1</sup>, Roukaerts Arnout <sup>13</sup>, Sanial Virginie  
15 <sup>5,25</sup>, Sauzède Raphaëlle <sup>26</sup>, Shelley Rachel U. <sup>1,27</sup>, Stewart Gillian <sup>28,29</sup>, Sutton Jill N. <sup>1</sup>, Tang Yi <sup>29,28</sup>,  
16 Tisnérat-Laborde Nadine <sup>15</sup>, Tonnard Manon <sup>1,30,31</sup>, Tréguer Paul <sup>1</sup>, van Beek Pieter <sup>5</sup>, Zurbrick  
17 Cheryl M. <sup>6</sup>, Zunino Patricia <sup>2</sup>

18

19 1 LEMAR (Laboratoire des Sciences de l'environnement marin), CNRS, Univ. Brest, IRD,  
20 Ifremer, Technopôle Brest-Iroise, 29280 Plouzané, France  
21 2 Ifremer, Univ. Brest, CNRS, IRD, Laboratoire d'Océanographie Physique et Spatiale (LOPS),  
22 IUEM, Plouzané, France  
23 3 GEOMAR Helmholtz Centre for Ocean Research Kiel, 24148 Kiel, Germany  
24 4 Instituto de Investigaciones Marinas, IIM-CSIC, Eduardo Cabello 6, 36208 Vigo, Spain  
25 5 LEGOS (Laboratoire d'Etudes en Géophysique et Océanographie Spatiales), Université de  
26 Toulouse, CNES, CNRS, IRD, UPS, 14 Avenue Edouard Belin, 31400 Toulouse, France  
27 6 Earth, Atmospheric and Planetary Sciences, Massachusetts Institute of Technology,  
28 Cambridge, MA 02139, USA  
29 7 Laboratory of Ion Beam Physics, Department of Earth Sciences, Institute of Geochemistry  
30 and Petrology, ETH-Zurich, Otto Stern Weg 5, Zurich, 8093, Switzerland  
31 8 Institut de Ciència i Tecnologia Ambientals & Departament de Física, Universitat Autònoma  
32 de Barcelona, Bellaterra, 08193, Spain  
33 9 *Currently at* Laboratoire des cycles géochimiques, Géosciences Marines, Centre Ifremer  
34 Bretagne  
35 10 Laboratório de Hidroquímica-IO/FURG, Rio Grande, Brazil  
36 11 ISTERRE, Université Grenoble Alpes, CS 40700, 38058 GRENOBLE Cedex 9, France  
37 12 CNRS, INSU, Division Technique Bâtiment IPEV - Centre Ifremer, Technopôle Brest-Iroise,  
38 CS 50074, 29280 Plouzané, France  
39 13 Analytical, Environmental and Geo-Chemistry, Vrije Universiteit Brussel, Pleinlaan 2, 1050,  
40 Brussels, Belgium  
41 14 Department of Earth Sciences, University of Oxford, South Parks Road, Oxford OX13AN, UK  
42 15 LSCE/IPSL--CEA-CNRS-UVSQ--Université Paris Saclay, F-91198 Cedex, France  
43 16 Department of Biology, Dalhousie University, Halifax, Nova Scotia, Canada, B3H 4R2

44 17 Uni Research Climate, Bjerknes Centre for Climate Research, Bergen 5008, Norway  
45 18 Ocean Sciences Department, School of Environmental Sciences, University of Liverpool,  
46 Liverpool, 11 L69 3GP, UK  
47 19 IUEM, UMS 3113, CNRS, Univ. Brest, IRD, Ifremer, Technopôle Brest Iroise, rue Dumont  
48 d'Urville, 29280 PLOUZANE  
49 20 Aix Marseille Université, CNRS/INSU, Université de Toulon, IRD, Mediterranean Institute of  
50 Oceanography UM 110, Marseille, France  
51 21 *Currently at* Department of Earth Sciences, Institute of Geochemistry and Petrology, ETH  
52 Zurich, Zürich, Switzerland  
53 22 School of Science. Edith Cowan University. 270 Joondalup Drive, Joondalup WA 6027.  
54 Australia  
55 23 Oceans Institute & Department of Physics. School of Physics, Mathematics and Computing.  
56 The University of Western Australia. Crawley, WA 6009. Australia  
57 24 *Currently at* Department of earth Sciences, Stellenbosch University, Stellenbosch, 7600,  
58 South Africa.  
59 25 *Currently at* Division of Marine Science, University of Southern Mississippi, 1020 Balch Blvd.  
60 Stennis Space Center, MS 39529, USA  
61 26 Sorbonne Universités, UPMC Univ Paris 06, CNRS, Laboratoire d'Océanographie de  
62 Villefranche (LOV), 06230 Villefranche-sur-Mer, France  
63 27 *Currently at* Earth, Ocean and Atmospheric Science, Florida State University, Tallahassee,  
64 Florida 32306, USA  
65 28 School of Earth and Environmental Sciences, Queens College, City University of New York,  
66 Flushing, USA  
67 29 Earth and Environmental Sciences, the Graduate Center, City University of New York, New  
68 York, USA  
69 30 Antarctic Climate and Ecosystem Cooperative Research Centre (ACE CRC), University of  
70 Tasmania, Private Bag 80, Hobart, TAS 7001, Australia  
71 31 Institute for Marine and Antarctic Studies, University of Tasmania, Hobart, TAS 7001,  
72 Australia

73

74

75

## 76 **Abstract**

77 The GEOVIDE cruise, a collaborative project within the framework of the international  
78 GEOTRACES programme, was conducted along the French-led section in the North Atlantic  
79 Ocean (Section GA01), between 15 May and 30 June 2014. In this Special Issue, results from  
80 GEOVIDE, including physical oceanography and trace element and isotope cyclings, are  
81 presented among seventeen articles. Here, the scientific context, project objectives and  
82 scientific strategy of GEOVIDE are provided, along with an overview of the main results from  
83 the articles published in the special issue.

84

85

86 **1. Scientific context and objectives**

87

88 Understanding the distribution, sources, and sinks of trace elements and isotopes (TEIs) will  
89 improve our ability to understand the past and present marine environments. Some TEIs are  
90 toxic (e.g. Hg), while others are essential micronutrients involved in many metabolic processes  
91 of marine organisms (e.g. Fe, Mn). The availability of TEIs therefore constrains the ocean  
92 carbon cycle and affects a range of other biogeochemical processes in the Earth system, whilst  
93 responding to and influencing global change (de Baar et al., 2005; Blain et al., 2007; Boyd et  
94 al., 2007; Pollard et al., 2007). Moreover, TEI interactions with the marine food web strongly  
95 depend on their physical (particulate/dissolved/colloidal/soluble) and chemical (organic and  
96 redox) forms. In addition, some TEIs are diagnostic in allowing the quantification of specific  
97 mechanisms in the marine environment that are challenging to measure directly. Few  
98 examples include: (i) atmospheric deposition (e.g.  $^{210}\text{Pb}$ , Al, Mn, Th isotopes,  $^7\text{Be}$ ; Baker et al.,  
99 2016; Hsieh et al., 2011; Measures and Brown, 1996), (ii) mixing rates of deep waters or shelf-  
100 to-open ocean (e.g.  $^{231}\text{Pa}/^{230}\text{Th}$ ,  $\Delta^{14}\text{C}$ , Ra isotopes,  $^{129}\text{I}$ ,  $^{236}\text{U}$ ; van Beek et al., 2008; Casacuberta  
101 et al., 2016; Key et al., 2004), (iii) boundary exchange processes (e.g.  $\epsilon_{\text{Nd}}$ , Jeandel et al., 2011;  
102 Lacan and Jeandel, 2001, 2005), and (iv) downward flux of organic carbon and/or  
103 remineralisation in deep waters (e.g.  $^{234}\text{Th}/^{238}\text{U}$ ,  $^{210}\text{Pb}/^{210}\text{Po}$ ,  $\text{Ba}_{\text{XS}}$ ; Buesseler et al., 2004;  
104 Dehairs et al., 1997; Roca-Martí et al., 2016). In such settings, TEIs provide chemical  
105 constraints and allow the estimation of fluxes which was not possible before the development  
106 of their analyses. Finally, paleoceanographers are wholly dependent on the development of  
107 tracers, many of which are based on TEIs used as proxies, in order to reconstruct past  
108 environmental conditions (e.g. ocean productivity, patterns and rates of ocean circulation,  
109 ecosystem structures, ocean anoxia; Henderson, 2002). Such reconstruction efforts are  
110 essential to assess the processes involved in regulating the global climate system, and possible  
111 future climate change variability.

112 Despite all these major implications, the distribution, sources, sinks, and internal cycling of  
113 TEIs in the oceans are still largely unknown due to the lack of appropriate clean sampling  
114 approaches and insufficient sensitivity and selectivity of the analytical measurement  
115 techniques until recently. This last point has improved very quickly as significant  
116 improvements in the instrumental techniques now allow the measurements of

117 concentrations, speciation (physical and chemical forms), and isotopic compositions for most  
118 of the elements of the periodic table which have been identified either as relevant tracers or  
119 key nutrients in the marine environment. These recent advances provide the marine  
120 geochemistry community with a significant opportunity to make substantial contributions to  
121 a better understanding of the marine environment.

122

123 In this general context, the aim of the international GEOTRACES programme is to  
124 characterize TEI distributions on a global scale, consisting of ocean sections, and regional  
125 process studies, using a multi-proxy approach. The GEOVIDE section is the French contribution  
126 to this global survey in the North Atlantic Ocean along the OVIDE section and in the Labrador  
127 Sea (Fig. 1) and complements a range of other international cruises in the North Atlantic.  
128 GEOVIDE leans on the knowledge gained by the OVIDE project during which the Portugal-  
129 Greenland section has been carried out biennially since 2002, gathering physical and  
130 biogeochemical data from surface to bottom (Mercier et al., 2015; Pérez et al., 2018).

131

132

#### 133 Rationale for the GEOVIDE section:

134 i) The North Atlantic Ocean plays a key role in mediating the climate of the Earth. It  
135 represents a key region of the Meridional Overturning Circulation (MOC) and a major sink of  
136 anthropogenic carbon ( $C_{\text{ant}}$ ) (Pérez et al., 2013; Sabine et al., 2004; Seager et al., 2002). Since  
137 2002, the OVIDE project has contributed to the observation of both the circulation and water  
138 mass properties of the North Atlantic Ocean. Despite the importance of the MOC on global  
139 climate, it is still challenging to assess its strength within a reasonable uncertainty (Kanzow et  
140 al., 2010; Lherminier et al., 2010). The MOC strength estimated from *in-situ* measurements on  
141 OVIDE cruises has thus helped to validate a time series for the amplitude of the MOC (based  
142 on altimetry and ARGO float array data) that exhibits a drop of  $2.5 \pm 1.4$  Sv (95% confidence  
143 interval) between 1993 and 2010 (Mercier et al., 2015), consistent with other modelling  
144 studies (Xu et al., 2013). This time series, along with the *in situ* data, shows a recovery of the  
145 MOC amplitude in 2014 at a value similar to those of the mid-1990s, confirming the  
146 importance of the decadal variability in the subpolar gyre. During OVIDE, the contribution of  
147 the most relevant currents, water masses and biogeochemical provinces have been localized

148 and quantified. This knowledge was crucial for the establishment of the best strategy to  
149 sample TEIs in this specific region.

150 In addition to the OVIDE section, the Labrador Sea section offered a unique opportunity to  
151 complement the MOC estimate, to analyse the propagation of anomalies in temperature and  
152 salinity (Reverdin et al., 1994), and to study the distribution of TEIs along the boundary current  
153 of the subpolar gyre, coupling both observations and modelling.

154 Moreover, recent results provided evidences that CO<sub>2</sub> uptake in the North Atlantic was  
155 reduced by the weakening of the MOC (Pérez et al., 2013). The most significant finding of this  
156 study was that the uptake of C<sub>ant</sub> occurred almost exclusively in the subtropical gyre, while  
157 natural CO<sub>2</sub> uptake dominated in the subpolar gyre. In light of these new results, one issue to  
158 be addressed was the coupling between the C<sub>ant</sub> and the transport of water, with the aim to  
159 understand how the changes in the ventilation and in the circulation of water masses affect  
160 the C<sub>ant</sub> uptake and its storage capacity in the various identified provinces (Fröb et al., 2018).

161 Finally, as the subpolar North Atlantic forms the starting point for the global ocean conveyor  
162 belt, it is of particular interest to investigate how TEIs are transferred to the deep ocean  
163 through both ventilation and particle sinking, and how deep convection processes impact the  
164 TEI distributions in this key region.

165

166 ii) A better assessment of the factors that control organic production and export of carbon  
167 in the productive North Atlantic Ocean, together with a better understanding of the role  
168 played by TEIs in these processes are research priorities. Pronounced phytoplankton blooms  
169 occur in the North Atlantic in spring in response to upwelling and water column  
170 destratification (Bury et al., 2001; Henson et al., 2009; Savidge et al., 1995). Such blooms are  
171 known to trigger substantial export of fast-sinking particles (Lampitt, 1985), and can represent  
172 a major removal mechanism for particulate organic carbon, macronutrients, and TEIs to the  
173 deep ocean.

174

175 iii) In the North Atlantic, TEI distributions are influenced by a variety of sources including, for  
176 the most important, the atmosphere and the margins (Iberian, Greenland, and Labrador  
177 margins).

178

179 *Atmosphere:* Atmospheric inputs (e.g. mineral dust, anthropogenic emission aerosols) are an  
180 important sources of TEIs to the North Atlantic Ocean due to the combined effects of  
181 anthropogenic emissions from industrial/agricultural sources and mineral dust mobilized from  
182 the arid regions of North Africa (Duce et al., 2008; Jickells et al., 2005). Model and satellite  
183 data for the GEOVIDE section suggested that an approximately tenfold decrease in the  
184 atmospheric concentrations of mineral dust was expected from south to north (Mahowald et  
185 al., 2005). As there had been relatively few aerosol TEI studies in the northern North Atlantic  
186 compared to the tropical and subtropical North Atlantic prior to GEOVIDE, constraining  
187 atmospheric deposition fluxes to this region had been identified as a research priority (de  
188 Leeuw et al., 2014). During the GEOVIDE campaign, a multi-proxy approach (e.g. aerosol trace  
189 element concentrations, dissolved and particulate Al and Mn, seawater  $^{210}\text{Pb}$ , Fe, Nd and Th  
190 isotopes,  $^7\text{Be}$ ) was taken to achieve the objective of better constraining the atmospheric  
191 deposition fluxes of key trace elements.

192

193 *Margins:* The continental shelves can act as a filter for TEIs supplied from shelf sediments,  
194 submarine groundwater discharge (including the discharge of fresh groundwater into the  
195 coastal seas and recirculation of seawater through the sediment), and rivers. While some TEIs  
196 are removed on the continental shelves, others are thought to be mobilized from the solid  
197 phase at the land-ocean interface (e.g. Fe and likely other micro- and macro-nutrients, such  
198 as Cu, Ni, Mn, and Si; Chase et al., 2005; Jeandel and Oelkers, 2015). The cruise track  
199 intersected several margins, thus allowing for the characterization of continental sources and  
200 quantification of TEI fluxes associated with these sources in various shelf regimes.

201

202 iv) It is obviously needed to further validate the use of paleo-proxies. For example, in recent  
203 years, the potential of the  $^{231}\text{Pa}/^{230}\text{Th}$  ratio for identifying past rates of ocean circulation, and  
204 of the isotopic composition of neodymium ( $\epsilon_{\text{Nd}}$ ) as a tracer of thermohaline circulation have  
205 led to many paradigm-changing results for the reconstitution of the Atlantic Ocean circulation  
206 (McManus et al., 2004; Montero-Serrano et al., 2013; Negre et al., 2010). However, there is  
207 an ongoing debate about the interpretation of  $^{231}\text{Pa}/^{230}\text{Th}$  paleo-records in the Atlantic (Hayes  
208 et al., 2015; Keigwin and Boyle, 2008) focused on the effects of particle fluxes versus those of  
209 water circulation. Only one single  $^{231}\text{Pa}$  profile in the Subpolar North Atlantic has been  
210 published before GEOVIDE (Moran et al., 2002). Regarding Nd isotopes, although several

211 profiles of dissolved (and total) Nd isotopes are available in the boundary currents of  
212 Greenland and the Labrador Sea, there are very few profiles for the ocean interior of the  
213 GEOVIDE region (Copard et al., 2011; Filippova et al., 2017; Lacan and Jeandel, 2004; Lambelet  
214 et al., 2016). In addition, the importance of dissolved/particle interactions in the control of  
215 the isotopic composition of Nd is becoming increasingly apparent. To our knowledge,  
216 particulate  $\epsilon_{Nd}$  data have not been published yet for the Subpolar North Atlantic. For these  
217 reasons, documenting these tracers in both dissolved and particulate phases is needed to  
218 provide new constraints and significantly advance our understanding of the cycles of these  
219 tracers and their use in the modern and past oceans.

220 Furthermore, proxies of nutrient utilization, such as the silicon stable isotopes ( $\delta^{30}Si$ ) from  
221 diatom silica, provides a means of reconstructing the behaviour of past geochemical cycles  
222 and the past strength of the biological pump, and its influence on atmospheric concentrations  
223 of  $CO_2$ . However, successful application of  $\delta^{30}Si$  in diatoms accumulating in sediments for  
224 reconstruction of past silica cycling requires a thorough understanding of  $\delta^{30}Si$  of dissolved Si  
225 ( $\delta^{30}Si_{Dsi}$ ) and of the processes that control its distribution throughout the modern ocean.  
226 Combining studies in the Southern Ocean (De La Rocha et al., 2011; Fripiat et al., 2011) and  
227 North and Equatorial Pacific (De La Rocha et al., 2000) with a global circulation model  
228 (Wischmeyer et al., 2003) has revealed the roles that ocean circulation and biogeochemical  
229 cycling play in controlling the distribution of silicon isotopes within the ocean. Largely missing  
230 from this dataset was the North Atlantic Ocean (De La Rocha et al., 2011).

231

232 In this general context, the main scientific objectives of GEOVIDE were to (i) better  
233 understand and quantify the MOC and the carbon cycle carbon cycle in the context of decadal  
234 variability, adding new tracers to this end, (ii) map the TEI distributions, including their physical  
235 and chemical speciation, along this full-depth high resolution ocean section, (iii) investigate  
236 the links between TEIs and the production, export, and remineralisation of particulate organic  
237 matter, (iv) identify TEI sources and sinks, and quantify their fluxes at the ocean boundaries,  
238 and (v) better understand and quantify the paleoproxies  $^{231}Pa/^{230}Th$ ,  $\epsilon_{Nd}$ , and  $\delta^{30}Si$ .

239

240

241 2. Strategy

242

243 To achieve the objectives of the GEOVIDE project, a 47-day multidisciplinary cruise was  
244 carried out on board R/V Pourquoi Pas? in the North Atlantic Ocean along the OVIDE section,  
245 from Lisbon to Greenland, and in the Labrador Sea (Fig. 1). The Labrador section was chosen  
246 according to the OSNAP (Overturning in the Subpolar North Atlantic Programme)  
247 recommendations because it transects the export route of the Labrador Sea Water  
248 downstream of its formation site. Therefore, the properties of the North Atlantic Deep Water  
249 (NADW) at 53°N are likely to be representative of NADW further south and a 15-year time  
250 series of currents and hydrographic properties is available in the Western Boundary Current  
251 at this latitude (Fischer et al., 2010). The GEOVIDE cruise took place from 15 May to 30 June  
252 2014, during the same season as the previous OVIDE cruises (2002-2012). The cruise timing  
253 helped to minimize seasonal variations and maximize the representativeness of inter-annual  
254 variability of the physical parameters investigated in this specific region. Furthermore, this  
255 period of the year corresponds to the bloom/post-bloom period of the subpolar gyre and post-  
256 bloom period in the sub-tropical gyre (Henson et al., 2005), thus allowing for the study of the  
257 complexity of the biological pump and the links between production, export of organic matter,  
258 and TEIs.

259 A high resolution hydrographical section that includes the *in-situ* measurements of the  
260 currents by doppler profilers was performed and, as recommended by GEOTRACES, a multi-  
261 proxy approach was used. In total, 78 stations were occupied (plus one test station). Station  
262 naming depended on the number of casts that were conducted: Short (47 one-cast stations),  
263 Large (17 three-cast stations), XLarge (5 five-cast stations), and Super (10 multi-cast stations).  
264 A total of 341 on-deck operations were carried out during GEOVIDE.

265 In total, (i) the standard stainless steel rosette was deployed 163 times, (ii) the trace metal  
266 clean rosette, 53 times, (iii) *in-situ* pumps, 25 times, (iv) the mono-corer, with or without *in-*  
267 *situ* pumps clamped on the cable, 11 times and (v) the plankton net, 9 times. We also collected  
268 140 surface seawater samples using a fish towed from the ship's starboard side and deployed  
269 at 1–2 m depth, 18 aerosol samples, and 10 rainwater samples. In addition, we deployed: 60  
270 expendable BathyThermographs (XBTs), 17 ARGO profiling floats (8 ARVOR, 2 ARVOR-deep, 2  
271 PROVOR-DO, 2 PROVBIO, 1 ARVOR double DO, and 2 APEX), and 12 weather buoys.

272

273

274 3. Summary of the main results published in this special issue



275

276 In this special issue, seventeen publications present results of the GEOVIDE project. Six other  
277 manuscripts have already been published in other journals (Benetti et al., 2017; Cossa et al.,  
278 2018b; Le Reste et al., 2016; Pérez et al., 2018; Shelley et al., 2017; Zunino et al., 2015). Due  
279 to the long time required for some analyses, other articles related to this project are to be  
280 expected for publication at a later date.

281 The articles in this special issue are linked to four general research themes: (i) hydrographic  
282 and physical characteristics, (ii) links between water masses and TEIs, (iii) external sources and  
283 sinks of TEIs, and (iv) biogeochemical tracers of community structure, export and  
284 remineralisation.

285

### 286 3.1. Hydrographic and physical characteristics

287 In terms of circulation, the comparison with the 2002–2012 mean state shows a different  
288 repartition of the northward warm currents that compose the upper limb of the MOC, with a  
289 more intense Irminger Current (station 39-41) and a weaker North Atlantic Current (NAC) in  
290 the Western European Basin, these anomalies being compatible with the variability previously  
291 observed along the OVIDE section in the 2000s (Zunino et al., 2017). The distribution of the  
292 volume transport in the three branches of the NAC (Fig. 1) has changed: no transport was  
293 found in the northern branch, although 11 Sv were found in the mean of the previous decade,  
294 and the central branch, that marks the limit between the subpolar and the subtropical regions,  
295 nearly doubled in 2014.

296 The main hydrographic properties along the GEOVIDE section are shown on Fig. 2 for  
297 potential temperature, salinity, dissolved oxygen, nitrate + nitrite, and silicic acid. The surface  
298 waters of the eastern SPNA, down to about 500 m, were much colder and fresher than the  
299 average values observed over 2002–2012 (Zunino et al., 2017). In the context of the ocean  
300 heat loss observed in the subpolar gyre since 2005, the year 2013-2014 was indeed particularly  
301 intense. Remarkably, despite the negative temperature anomalies in the surface waters, the  
302 heat transport across the OVIDE section estimated during GEOVIDE was the largest measured  
303 since 2002. This was attributed to the relatively strong MOC measured across the OVIDE  
304 section during GEOVIDE (Zunino et al., 2017) and more particularly to the strong transport of  
305 central water in the central and southern branch of the NAC (García-Ibáñez et al., 2018) that  
306 compensates the cold anomaly of the surface layer. The relatively strong MOC and heat

307 transport were confirmed by Holliday et al. (2018) across a nearly simultaneous section (June-  
308 July 2014) between Labrador and Scotland.

309 The water mass properties of the GEOVIDE cruise were used to perform an extended  
310 Optimum MultiParameter (eOMP) analysis and to assess the water mass distribution (García-  
311 Ibáñez et al., 2018). The eOMP analysis together with the absolute geostrophic velocity field  
312 determined using a box inverse model allowed the evaluation of the relative importance of  
313 each water mass to the MOC. The increase in the MOC intensity from 2002–2010 to 2014 was  
314 shown to be related to the increase in the northward transport of the Central Waters in its  
315 upper limb (from the surface to 1000 m in the south-eastern part of the section), and in the  
316 southward flow of both the Subpolar Mode Water of the Irminger Basin (SPMW, 200 to  
317 1500 m) and the Iceland–Scotland Overflow Water (ISOW, between 1800 and 3000 m) in its  
318 lower limb (García-Ibáñez et al., 2018).

319 In addition, the precise determination of different water masses (García-Ibáñez et al., 2018)  
320 and ventilation processes are crucial for the interpretation of the TEIs whose distributions are,  
321 for many of them, strongly related to water masses.

322

### 323 3.2. Links between water masses and TEIs

324 The concentrations of TEIs are strongly influenced by water mass distribution, age, and  
325 circulation/mixing. For instance, this is the case of  $^{230}\text{Th}$  and  $^{231}\text{Pa}$ , high concentrations of both  
326 tracers were observed in the old water of North East Atlantic Deep Water (NEADW), and low  
327 values in young waters, particularly in Denmark Strait Overflow Water (DSOW) (Deng et al.,  
328 2018). The low values of  $^{230}\text{Th}$  and  $^{231}\text{Pa}$  in water near the seafloor of the Labrador and  
329 Irminger Seas are related to the young waters present in those regions (Deng et al., 2018).  
330 This study reports systematic increase of  $^{230}\text{Th}$  activities with water age but a more complex  
331 relationship between age and  $^{231}\text{Pa}$  which challenges some approaches to the use of  
332 sedimentary  $^{231}\text{Pa}/^{230}\text{Th}$  ratios to assess past rates of oceanic circulation. The application of  
333 this proxy at a basin scale to constrain the overturning circulation is, however, supported by  
334 GEOVIDE data which now allows a complete nuclide budget for the North Atlantic to be  
335 constructed (Deng et al., 2018).

336 Long-lived artificial radionuclides were also very useful to assess the circulation in the  
337 SPNA, namely  $^{129}\text{I}$  and  $^{236}\text{U}$ , and the origin of water masses in a dual tracer approach (i.e.  
338  $^{129}\text{I}/^{236}\text{U}$  and  $^{236}\text{U}/^{238}\text{U}$  atom ratios) (Castrillejo et al., 2018). These transient tracers, originating

339 from La Hague (France) and Sellafield (UK) nuclear reprocessing plants and the atmospheric  
340 nuclear weapon tests, helped investigating the shallow western boundary transport and the  
341 ventilation processes. For example, the  $^{129}\text{I}$  concentrations validate the ISOW transport  
342 pathways in the Western European basin. The time series of  $^{129}\text{I}$  in the Labrador Sea revealed  
343 two circulation loops of the Atlantic Waters carrying the signal from the European  
344 reprocessing plants: i) a short loop through the Nordic Seas into the central Labrador Sea of  
345 about 8-10 years, and; ii) a longer loop which includes about 8 additional years of recirculation  
346 in the Arctic Eurasian Basin before entering back to the Atlantic Ocean (Castrillejo et al., 2018).

347 Some other TEIs were also strongly linked to water mass distribution: Within GEOVIDE,  
348 silicon isotopes (Sutton et al., 2018), lead (Pb) (Zurbrick et al., 2018), mercury (Hg) (Cossa et  
349 al., 2018a), and particulate and dissolved Fe and Al (Gourain et al., 2018; Menzel Barraqueta  
350 et al., 2018a; Tonnard et al., 2018), as examples. For instance, the Labrador Seawater (LSW) is  
351 characterized by a relatively high silicon stable isotope composition for dissolved silicon  
352 ( $\delta^{30}\text{Si}_{\text{DSi}}$ ) whose signature can be seen not only in the region where it is formed, but also  
353 throughout the mid-depth zone of the North Atlantic Ocean (Sutton et al., 2018). The  $\delta^{30}\text{Si}_{\text{DSi}}$   
354 distribution thus provides information on the interaction between subpolar/polar water  
355 masses of northern and southern origin, and indicates the extent to which local signatures are  
356 influenced by source waters (Sutton et al., 2018). In LSW, the concentrations of Pb (Zurbrick  
357 et al., 2018) and Hg (Cossa et al., 2018a) provided evidence for a decrease in the  
358 anthropogenic inputs of these two elements over the last decade, since the values are lower  
359 in the recently formed LSW between Greenland and Newfoundland than in the older LSW of  
360 the Western European basin.

361 The Mediterranean Water (MW), meanwhile, was characterised by higher concentrations  
362 of trace metals, such as Pb, Hg, and Al (Cossa et al., 2018a; Menzel Barraqueta et al., 2018a;  
363 Zurbrick et al., 2018). It reflects the importance of Saharan and anthropogenic atmospheric  
364 inputs to the Mediterranean region, which are much higher than in our studied area (see  
365 below), as well as enhanced remineralisation as indicated by the correlation between total  
366 mercury concentrations and the apparent oxygen utilisation (Cossa et al., 2018a).

367

### 368 3.3. TEI sources and sinks

369 Different methods/TEIs were used to estimate atmospheric input fluxes: aerosol  
370 concentrations in aerosol and rainwater samples were compared with estimates derived from

371 the measurement of beryllium-7 ( $^7\text{Be}$ ) in aerosols, rainwater and seawater (Shelley et al.,  
372 2017). Taking a different approach, Menzel Barraqueta et al. (2018b) used dAl in the surface  
373 waters to estimate the atmospheric input flux. All these methods allowed concluding that the  
374 atmospheric inputs of total trace elements were low in our study area, and the soluble input  
375 was even lower, based on their fractional solubility (Shelley et al., 2018).

376 One of the main sources of TEIs during GEOVIDE was sediment input (i) within the benthic  
377 nepheloid layers in the Iceland, Irminger and Labrador Basins (Gourain et al., 2018), and (ii)  
378 above the Iberian, Greenland and Canadian margins, as well as fluvial and meteoric inputs  
379 (Benetti et al., 2017). This is notably the case for some dissolved TEIs, such as Fe (Tonnard et  
380 al., 2018), Al (Menzel Barraqueta et al., 2018a), and radium-226 ( $^{226}\text{Ra}$ ) or barium (Ba) (Le Roy  
381 et al., 2018), as well as for particulate trace elements (Gourain et al., 2018). Overall, enhanced  
382 concentrations of TEIs close to the bottom suggest that continental shelves and margins acted  
383 as a source to adjacent waters. In the case of the Iberian margin, advection of particulate Fe  
384 (pFe) was visible over a distance of more than 250 km from the source (Gourain et al., 2018).

385 However, some results provide evidence that occasional removal of dFe or dAl by particles  
386 can be a dominant process rather than partial dissolution from resuspended sediments, but  
387 this is likely dependent on the nature of particles (Menzel Barraqueta et al., 2018a).

388 Additional sources for particulate elements and sinks for dissolved ones are biological  
389 uptake and scavenging. Evidence for a biogenic influence on the pFe/pAl ratios within the  
390 Irminger and Labrador Basins was found by Gourain et al. (2018). Almost all the stations  
391 displayed dFe minima in surface waters, in association with the chlorophyll maxima. The  
392 abundance of diatoms exerted a significant control on the surface concentrations of Fe and Al  
393 (Menzel Barraqueta et al., 2018b; Tonnard et al., 2018). Remineralisation processes were also  
394 highlighted for some TEIs (see also section 3.4). Dissolved Al concentrations generally  
395 increased with depth and the net release of dAl at depth during remineralisation of sinking  
396 biogenic opal containing particles was generally larger than the net removal of dAl through  
397 scavenging.

398

#### 399 3.4. Production, export, and remineralisation

400 The main biogeochemical features of the GEOVIDE cruise in terms of biogenic silica (BSi),  
401 particulate organic carbon (POC), and particulate organic nitrogen (PON) are reported on Fig.  
402 3 and supplementary material. The highest BSi concentrations were observed in the Irminger

403 and Labrador Seas. POC and PON were also high in these regions, but also show high values in  
404 the Iceland and Western European Basins.

405 On the Iberian margin and in the Western European Basin, an unexpectedly high  
406 heterotrophic nitrogen fixation activity was reported, likely sustained by the availability of  
407 phytoplankton-derived organic matter (dissolved and/or particulate), resulting from the on-  
408 going to post spring bloom conditions, while dissolved iron supply relied on atmospheric  
409 deposition and surface waters advection from the subtropical region and the shelf area  
410 (Fonseca-Batista et al., 2018).

411 In terms of particulate organic carbon (POC) export, thorium-234 ( $^{234}\text{Th}$ ) was used to  
412 provide estimates of POC export fluxes, with the highest values near the Iberian margin where  
413 a phytoplankton bloom was declining, and the lowest values in the Irminger Basin where the  
414 bloom was close to its maximum (Lemaitre et al., 2018a). The proxy  $^{210}\text{Po}/^{210}\text{Pb}$  was also used  
415 to assess the export of particles (Tang et al., 2018). The prominent role of small particles in  
416 sorption was confirmed, suggesting that particulate radionuclide activities and export of both  
417 small (1-53  $\mu\text{m}$ ) and large (> 53  $\mu\text{m}$ ) particles should be considered to account for the observed  
418 surface water  $^{210}\text{Po}/^{210}\text{Pb}$  disequilibria (Tang et al., 2018).

419 In the subpolar and subtropical regions, the mesopelagic POC remineralisation fluxes,  
420 estimated from the particulate biogenic barium (excess barium;  $\text{Ba}_{\text{xs}}$ ) proxy, were found to be  
421 equal to and occasionally higher than the upper ocean POC export fluxes (Lemaitre et al.,  
422 2018b). These results highlighted the strong impact of the mesopelagic remineralisation on  
423 the biological carbon pump with a very low carbon sequestration efficiency at the time of our  
424 study (Lemaitre et al., 2018b).

425

426

## 427 **Conclusion**

428 The main GEOVIDE results have helped to improve our understanding of the TEI cycles in the  
429 North Atlantic. The strong physical oceanography background of the GEOVIDE project is a  
430 strength for interpreting our data. For many TEIs, a strong link was observed between their  
431 distributions and water masses. On the other hand, TEIs also helped to constrain oceanic  
432 circulation, notably in the subpolar gyre and Labrador Sea. Important sources (sediments,  
433 fluvial, and meteoric) and sinks (biological uptake and scavenging) of TEIs were highlighted.

434 The biological carbon pump was studied and showed different efficiencies in the various  
435 studied regions.

436

#### 437 **Acknowledgements:**

438 We are greatly thankful to the captain, Gilles Ferrand, and crew of the N/O Pourquoi Pas?  
439 for their help during the GEOVIDE mission. This work was supported by the French National  
440 Research Agency (ANR-13-BS06-0014, ANR-12-PDOC-0025-01), the French National Centre for  
441 Scientific Research (CNRS-LEFE-CYBER), the LabexMER (ANR-10-LABX-19), and Ifremer. It was  
442 supported for the logistic by DT-INSU and GENAVIR.

443

#### 444 **References**

445 de Baar, H. J. W., Boyd, P. X., Coale, K. H., Landry, M. R., Tsuda, A., Assmy, P., Bakker, D. C. E., Bozec,  
446 Y., Barber, R. T., Brzezinski, M. A., Buesseler, K. O., Boye, M., Croot, P. L., Gervais, F., Gorbunov,  
447 M. Y., Harrison, P. J., Hiscock, W. T., Laan, P., Lancelot, C., Law, C. S., Levasseur, M., Marchetti, A.,  
448 Millero, F., Nishioka, J., Nojiri, Y., van Oijen, T., Riebesell, U., Rijkenberg, M. J. A., Saito, H., Takeda,  
449 S., Timmermans, K. R., Veldhuis, M. J. W., Waite, A. M. and Wong, C.-S.: Synthesis of iron  
450 fertilization experiments: From the Iron Age in the Age of Enlightenment, *J Geophys Res*, 110,  
451 C09S16, doi:10.1029/2004JC002601, 2005.

452 Baker, A. R., Landing, W. F., Bucciarelli, E., Cheize, M., Fietz, S., Hayes, C. T., Kadko, D., Morton, P. L.,  
453 Rogan, N., Sarthou, G., Shelley, R. U., Shi, Z., Shiller, A. M. and Van Hulten, M. M. P.: Air - Sea  
454 Deposition of Trace Elements | *Philosophical Transactions of the Royal Society of London A:*  
455 *Mathematical, Physical and Engineering Sciences*, [online] Available from:  
456 <http://rsta.royalsocietypublishing.org/content/374/2081/20160190> (Accessed 18 June 2018),  
457 2016.

458 van Beek, P., Bourquin, M., J.-L., R., Souhaut, M., Charette, M. A. and Jeandel, C.: Radium isotopes to  
459 investigate the water mass pathways on the Kerguelen Plateau (Southern Ocean), *Deep Sea Res*  
460 II, 55(5–7), 622–637, 2008.

461 Benetti, M., Reverdin, G., Lique, C., Yashayaev, I., Holliday, N. P., Tynan, E., Torres-Valdes, S.,  
462 Lherminier, P., Tréguer, P. and Sarthou, G.: Composition of freshwater in the spring of 2014 on  
463 the southern Labrador shelf and slope, *J. Geophys. Res. Oceans*, 122(2), 1102–1121,  
464 doi:10.1002/2016JC012244, 2017.

465 Blain, S., Quéguiner, B., Armand, L., Belviso, S., Bombled, B., Bopp, L., Bowie, A., Brunet, C., Brussaard,  
466 C., Carlotti, F., Christaki, U., Corbière, A., Durand, I., Ebersbach, F., Fuda, J.-L., Garcia, N., Gerringa,  
467 L., Griffiths, B., Guigue, C., Guillerm, C., Jacquet, S., Jeandel, C., Laan, P., Lefèvre, D., Lomonaco,  
468 C., Malits, A., Mosseri, J., Obernosterer, I., Park, Y.-H., Picheral, M., Pondaven, P., Remenyi, T.,  
469 Sandroni, V., Sarthou, G., Savoye, N., Scouarnec, L., Souhaut, M., Thuiller, D., Timmermans, K.,  
470 Trull, T., Uitz, J., van-Beek, P., Veldhuis, M., Vincent, D., Viollier, E., Vong, L. and Wagener, T.:  
471 Impact of natural iron fertilization on carbon sequestration in the Southern Ocean, *Nature*, 7139,  
472 1070–1074, 2007.

473 Boyd, P. W., Jickells, T., Law, C. S., Blain, S., Boyle, E. A., Buesseler, K. O., Coale, K. H., Cullen, J. J., Baar,  
474 H. J. W. de, Follows, M., Harvey, M., Lancelot, C., Levasseur, M., Owens, N. P. J., Pollard, R., Rivkin,  
475 R. B., Sarmiento, J., Schoemann, V., Smetacek, V., Takeda, S., Tsuda, A., Turner, S. and Watson, A.  
476 J.: Mesoscale Iron Enrichment Experiments 1993–2005: Synthesis and Future Directions, *Science*,  
477 315, 612–617, 2007.

478 Buesseler, K. O., Andrews, J. E., Pike, S. M. and Charette, M. A.: The effects of iron fertilization on  
479 carbon sequestration in the Southern Ocean, *Science*, 304(5669), 414–417, 2004.

480 Bury, S. J., Boyd, P. W., Preston, T., Savidge, G. and Owens, N. J. P.: Size-fractionated primary  
481 production and nitrogen uptake during a North Atlantic phytoplankton bloom : implications for  
482 carbon export estimates, *Deep Sea Res. Part 1 Oceanogr. Res. Pap.*, 48(3), 689–720; 7, 2001.

483 Casacuberta, N., Masqué, P., Henderson, G., Rutgers van-der-Loeff, M., Bauch, D., Vockenhuber, C.,  
484 Daraoui, A., Walther, C., Synal, H.-A. and Christl, M.: First  $^{236}\text{U}$  data from the Arctic Ocean and  
485 use of  $^{236}\text{U}/^{238}\text{U}$  and  $^{129}\text{I}/^{236}\text{U}$  as a new dual tracer, *Earth Planet. Sci. Lett.*, 440, 127–134,  
486 doi:10.1016/j.epsl.2016.02.020, 2016.

487 Castrillejo, M., Casacuberta, N., Christl, M., Vockenhuber, C., Synal, H.-A., García-Ibáñez, M. I.,  
488 Lherminier, P., Sarthou, G., Garcia-Orellana, J. and Masqué, P.: Tracing water masses with  $^{129}\text{I}$  and  
489  $^{236}\text{U}$  in the subpolar North Atlantic along the GEOTRACES GA01 section, *Biogeosciences*, 15(18),  
490 5545–5564, doi:https://doi.org/10.5194/bg-15-5545-2018, 2018.

491 Chase, Z., Johnson, K. S., Elrod, V. A., Plant, J. N., Fitzwater, S. E., Pickella, L. and Sakamoto, C. M.:  
492 Manganese and iron distributions off central California influenced by upwelling and shelf width,  
493 *Mar Chem*, 95, 235–254, 2005.

494 Copard, K., Colin, C., Frank, N., Jeandel, C., Montero-Serrano, J. C., Reverdin, G. and Ferron, B.: Nd  
495 isotopic composition of water masses and dilution of the Mediterranean outflow along the  
496 southwest European margin, *Geochem Geophys Geosyst*, 12, Q06020, 10.1029/2011GC003529,  
497 2011.

498 Cossa, D., Heimbürger, L.-E., Pérez, F. F., García-Ibáñez, M. I., Sonke, J. E., Planquette, H., Lherminier,  
499 P., Boutorh, J., Cheize, M., Menzel Barraqueta, J. L., Shelley, R. and Sarthou, G.: Mercury  
500 distribution and transport in the North Atlantic Ocean along the GEOTRACES-GA01 transect,  
501 *Biogeosciences*, 15(8), 2309–2323, doi:10.5194/bg-15-2309-2018, 2018a.

502 Cossa, D., Heimbürger, L. E., Sonke, J. E., Planquette, H., Lherminier, P., García-Ibáñez, M. I., Pérez, F.  
503 F. and Sarthou, G.: Sources, cycling and transfer of mercury in the Labrador Sea (Geotraces-  
504 Geovide cruise), *Mar. Chem.*, 198, 64–69, doi:10.1016/j.marchem.2017.11.006, 2018b.

505 Danialt, N., Mercier, H., Lherminier, P., Sarafanov, A., Falina, A., Zunino, P., Pérez, F. F., Ríos, A. F.,  
506 Ferron, B., Huck, T., Thierry, V. and Gladyshev, S.: The northern North Atlantic Ocean mean  
507 circulation in the early 21st century, *Prog. Oceanogr.*, 146, 142–158,  
508 doi:10.1016/j.pocean.2016.06.007, 2016.

509 De La Rocha, C. L., Hutchins, D. A., Brzezinski, M. A. and Zhang, Y.: Effects of iron and zinc deficiency  
510 on elemental composition and silica production by diatoms, *Mar Ecol Progr Ser*, 195, 71–79, 2000.

511 De La Rocha, C. L., Bescont, P., Croguennoc, A. and Ponzevera, E.: The silicon isotopic composition of  
512 surface waters of the Atlantic and Indian sectors of the Southern Ocean, *Geochim. Cosmochim.*  
513 *Acta*, 75, 5283–5295, 2011.

514 Dehairs, F., Shopova, D., Ober, S., Veth, C. and Goeyens, L.: Particulate barium stocks and oxygen  
515 consumption in the Southern Ocean mesopelagic water column during spring and early summer:  
516 relationship with export production, *Deep Sea Res. Part II Top. Stud. Oceanogr.*, 44(1), 497–516,  
517 doi:10.1016/S0967-0645(96)00072-0, 1997.

518 Deng, F., Henderson, G. M., Castrillejo, M. and Perez, F. F.: Evolution of  $^{231}\text{Pa}$  and  $^{230}\text{Th}$  in overflow  
519 waters of the North Atlantic, *Biogeosciences Discuss*, 1–24, doi:10.5194/bg-2018-191, in review,  
520 2018.

521 Duce, R. A., LaRoche, J., Altieri, K., Arrigo, K. R., Baker, A. R., Capone, D. G., Cornell, S., Dentener, F.,  
522 Galloway, J., Ganeshram, R. S., Geider, R. J., Jickells, T., Kuypers, M. M., Langlois, R., Liss, P. S., Liu,  
523 S. M., Middelburg, J. J., Moore, C. M., Nickovic, S., Oschlies, A., Pedersen, T., Prospero, J., Schlitzer,  
524 R., Seitzinger, S., Sorensen, L. L., Uematsu, M., Ulloa, O., Voss, M., Ward, B. and Zamora, L.:  
525 Impacts of atmospheric anthropogenic nitrogen on the open ocean, *Science*, 320(5878), 893–897,  
526 doi:10.1126/science.1150369, 2008.

527 Filippova, A., Frank, M., Kienast, M., Rickli, J., Hathorne, E., Yashayaev, I. M. and Pahnke, K.: Water  
528 mass circulation and weathering inputs in the Labrador Sea based on coupled Hf–Nd isotope

529 compositions and rare earth element distributions, *Geochim. Cosmochim. Acta*, 199, 164–184,  
530 doi:10.1016/j.gca.2016.11.024, 2017.

531 Fischer, J., Visbeck, M., Zantopp, R., Nunes, N. and doi:: Interannual to decadal variability of outflow  
532 from the Labrador Sea, *Geophys Res Lett*, 37, L24610, doi:10.1029/2010GL045321, 2010.

533 Fonseca-Batista, D., Li, X., Riou, V., Michotey, V., Fripiat, F., Deman, F., Guasco, S., Brion, N., Lemaitre,  
534 N., Tonnard, M., Gallinari, M., Planchon, F., Planquette, H., Sarthou, G., Elskens, M., Laroche, J.,  
535 Chou, L. and Dehairs, F.: Evidence of high N<sub>2</sub> fixation rates in productive waters of the temperate  
536 Northeast Atlantic, *Biogeosciences Discuss*, <https://doi.org/10.5194/bg-2018-220>, in review,  
537 2018.

538 Fripiat, F., Cavagna, A.-J., Nicolas, S., Dehairs, F., Andre, L. and Cardinal, D.: Isotopic constraints on the  
539 Si-biogeochemical cycle of the Antarctic Zone in the Kerguelen area (KEOPS), *Mar Chem*, 123(1–  
540 4), 11–22, DOI: 10.1016/j.marchem.2010.08.005, 2011.

541 Fröb, F., Olsen, A., Pérez, F. F., García-Ibáñez, M. I., Jeansson, E., Omar, A. and Lauvset, S. K.: Inorganic  
542 carbon and water masses in the Irminger Sea since 1991, *Biogeosciences*, 15(1), 51–72,  
543 doi:10.5194/bg-15-51-2018, 2018.

544 García-Ibáñez, M. I., Pérez, F. F., Lherminier, P., Zunino, P., Mercier, H. and Tréguer, P.: Water mass  
545 distributions and transports for the 2014 GEOVIDE cruise in the North Atlantic, *Biogeosciences*,  
546 15(7), 2075–2090, doi:10.5194/bg-15-2075-2018, 2018.

547 Gourain, A., Planquette, H., Cheize, M., Lemaitre, N., Menzel Barraqueta, J.-L., Shelley, R., Lherminier,  
548 P. and Sarthou, G.: Inputs and processes affecting the distribution of particulate iron in the North  
549 Atlantic along the GEOVIDE (GEOTRACES GA01) section, *Biogeosciences Discuss*, 1–42,  
550 doi:10.5194/bg-2018-234, 2018.

551 Hayes, C. T., Anderson, R. F., Fleisher, M. Q., Huang, K.-F., Robinson, L. F., Lu, Y., Cheng, H., Edwards,  
552 R. L. and Moran, S. B.: 230Th and 231Pa on GEOTRACES GA03, the U.S. GEOTRACES North Atlantic  
553 transect, and implications for modern and paleoceanographic chemical fluxes, *Deep Sea Res. Part*  
554 *II Top. Stud. Oceanogr.*, 116, 29–41, doi:10.1016/j.dsr2.2014.07.007, 2015.

555 Henderson, G. M.: New oceanic proxies for paleoclimate, *Earth Planet Sci Lett*, 203, 1–13, 2002.

556 Henson, S. A., Dunne, J. P. and Sarmiento, J. L.: Decadal variability in North Atlantic phytoplankton  
557 blooms, *J Geophys Res*, 114, C04013, doi:10.1029/2008JC005139, 2009.

558 Holliday, N. P., Bacon, S., Cunningham, S. A., Gary, S. F., Karstensen, J., King, B. A., Li, F. and Mcdonagh,  
559 E. L.: Subpolar North Atlantic Overturning and Gyre-Scale Circulation in the Summers of 2014 and  
560 2016, *J. Geophys. Res. Oceans*, 123(7), 4538–4559, doi:10.1029/2018JC013841, 2018.

561 Hsieh, Y.-T., Henderson, G. M. and Thomas, A. L.: Combining seawater 232Th and 230Th concentrations  
562 to determine dust fluxes to the surface ocean, *Earth Planet Sci. Lett*, 312, 280–290,  
563 doi:10.1016/j.epsl.2011.10.022, 2011.

564 Jeandel, C. and Oelkers, E. H.: The influence of terrigenous particulate material dissolution on ocean  
565 chemistry and global element cycles, *Chem. Geol.*, 395, 50–66,  
566 doi:10.1016/j.chemgeo.2014.12.001, 2015.

567 Jeandel, C., Peucker Ehrenbrink, B., Jones, M., Pearce, C., Oelkers, E., Godderis, Y., Lacan, F., Aumont,  
568 O. and Arsouze, T.: Ocean margins: the missing term for oceanic element budgets?, *EOS*, 92, 217–  
569 219, 2011.

570 Jickells, T. D., An, Z. S., Andersen, K. K., Baker, A. R., Bergametti, G., Brooks, N., Cao, J. J., Boyd, P. W.,  
571 Duce, R. A., Hunter, K. A., Kawahata, H., Kubilay, N., La Roche, J., Liss, P. S., Mahowald, N.,  
572 Prospero, J. M., Ridgwell, A. J., Tegen, I. and Torres, R.: Global Iron Connections Between Desert  
573 Dust, Ocean Biogeochemistry, and Climate, *Science*, 308, 67–71, 2005.

574 Kanzow, T., Cunningham, S. A., Johns, W. E., Hirschi, J. J.-M., Marotzke, J., Baringer, M. O., Meinen, C.  
575 S., Chidichimo, M. P., Atkinson, C., Beal, L. M., Bryden, H. L. and Collins, J.: Seasonal Variability of  
576 the Atlantic Meridional Overturning Circulation at 26.5°N, *J Clim.*, 23, 5678–5698,  
577 doi:10.1175/2010JCLI3389.1, 2010.

578 Keigwin, L. D. and Boyle, E. A.: Did North Atlantic overturning halt 17,000 years ago?,  
579 *Paleoceanography*, 23(1), doi:10.1029/2007PA001500, 2008.



580 Key, R. M., Kozyr, A., Sabine, C. L., Lee, K., Wanninkhof, R., Bullister, J. L., Feely, R. A., Millero, F. J.,  
581 Mordy, C. and Peng, T.-H.: A global ocean carbon climatology: Results from the Global Data  
582 Analysis Project (GLODAP), *Glob. Biogeochem Cycles*, 18, 10.1029/2004GB002247, 2004.

583 Lacan, F. and Jeandel, C.: Tracing Papua New Guinea imprint on the central Equatorial Pacific Ocean  
584 using neodymium isotopic compositions and Rare Earth Element patterns, *Earth Planet Sci Lett*,  
585 5779, 1–16, 2001.

586 Lacan, F. and Jeandel, C.: Subpolar Mode Water formation traced by neodymium isotopic composition,  
587 *Geophys. Res. Lett.*, 31, L14306, doi:10.1029/2004GL019747, 2004, 2004.

588 Lacan, F. and Jeandel, C.: Neodymium isotopes as a new tool for quantifying exchange fluxes at the  
589 continent-ocean interface, *Earth Planet Sci Lett*, 232(3–4), 245–257,  
590 doi:10.1016/j.epsl.2005.01.004, 2005.

591 Lambelet, M., van de Flierdt, T., Crocket, K., Rehkämper, M., Kreissig, K., Coles, B., Rijkenberg, M. J. A.,  
592 Gerringa, L. J. A., de Baar, H. J. W. and Steinfeldt, R.: Neodymium isotopic composition and  
593 concentration in the western North Atlantic Ocean: Results from the GEOTRACES GA02 section,  
594 *Geochim. Cosmochim. Acta*, 177(Supplement C), 1–29, doi:10.1016/j.gca.2015.12.019, 2016.

595 Lampitt, R. S.: Evidence for the seasonal deposition of detritus to the deep-sea floor and its subsequent  
596 resuspension, *Deep Sea Res I*, 32(8), 885–897, 1985.

597 Le Reste, S., Dutreuil, V., André, X., Thierry, V., Renaut, C., Le Traon, P.-Y. and Maze, G.: “Deep-Arvor”:  
598 A New Profiling Float to Extend the Argo Observations Down to 4000-m Depth, *J. Atmospheric  
599 Ocean. Technol.*, 33(5), 1039–1055, doi:10.1175/JTECH-D-15-0214.1, 2016.

600 Le Roy, E., Sanial, V., Charette, M. A., Beek, P. van, Lacan, F., Jacquet, S. H. M., Henderson, P. B.,  
601 Souhaut, M., García-Ibáñez, M. I., Jeandel, C., Pérez, F. F. and Sarthou, G.: The <sup>226</sup>Ra–Ba  
602 relationship in the North Atlantic during GEOTRACES-GA01, *Biogeosciences*, 15(9), 3027–3048,  
603 doi:https://doi.org/10.5194/bg-15-3027-2018, 2018.

604 de Leeuw, G., Guieu, C., Arneth, A., Bellouin, N., Bopp, L., Boyd, P. W., Denier van der Gon, H. A. C.,  
605 Desboeufs, K. V., Dulac, F., Facchini, M. C., Gantt, B., Langmann, B., Mahowald, N. M., Marañón,  
606 E., O’Dowd, C., Olgun, N., Pulido-Villena, E., Rinaldi, M., Stephanou, E. G. and Wagener, T.: Ocean–  
607 atmosphere interactions of particles, in *Ocean–Atmosphere Interactions of Gases and Particles*,  
608 edited by M. T. Johnson, pp. 171–246, DOI 10.1007/978-3-642-25643-1\_4, Springer: Heidelberg.,  
609 2014.

610 Lemaitre, N., Planchon, F., Planquette, H., Dehairs, F., Fonseca-Batista, D., Roukaerts, A., Deman, F.,  
611 Tang, Y., Mariez, C. and Sarthou, G.: High variability of export fluxes along the North Atlantic  
612 GEOTRACES section GA01: Particulate organic carbon export deduced from the 234Th method,  
613 *Biogeosciences Discuss*, 1–38, doi:10.5194/bg-2018-190, 2018a.

614 Lemaitre, N., Planquette, H., Planchon, F., Sarthou, G., Jacquet, S., García-Ibáñez, M. I., Gourain, A.,  
615 Cheize, M., Monin, L., André, L., Laha, P., Terryn, H. and Dehairs, F.: Particulate barium tracing of  
616 significant mesopelagic carbon remineralisation in the North Atlantic, *Biogeosciences*, 15(8),  
617 2289–2307, doi:10.5194/bg-15-2289-2018, 2018b.

618 Lherminier, P., Mercier, H., Huck, T., Gourcuff, C., Perez, F. F., Morin, P. and Sarafanov, A.: The Atlantic  
619 meridional overturning circulation and the subpolar gyre observed at the A25-Ovide section in  
620 June 2002 and 2004, *Deep Sea Res I*, 57(11), 1374–1391, doi:10.1016/j.dsr.2010.07.009, 2010.

621 Mahowald, N. M., Baker, A. R., Bergametti, G., Brooks, N., Duce, R. A., Jickells, T. D., Kubilay, N.,  
622 Prospero, J. M. and Tegen, I.: Atmospheric global dust cycle and iron inputs to the ocean, *Glob.  
623 Biogeochem Cy*, 19, GB4025, doi:10.1029/2004GB002402., 2005.

624 McManus, J. F., Francois, R., Gherardi, J.-M., Keigwin, L. D. and Brown-Leger, S.: Collapse and rapid  
625 resumption of Atlantic meridional circulation linked to deglacial climate changes, *Nature*, 428,  
626 834–837, 2004.

627 Measures, C. I. and Brown, E. T.: Estimating dust input to the Atlantic Ocean using surface water Al  
628 concentrations, in *The impact of African Dust across the Mediterranean*, edited by Guerzoni and  
629 Chester, p. 389, Kluwer., 1996.

630 Menzel Barraqueta, J.-L., Schlosser, C., Planquette, H., Gourain, A., Cheize, M., Boutorh, J., Shelley, R.,  
631 Contreira Pereira, L., Gledhill, M., Hopwood, M. J., Lacan, F., Lherminier, P., Sarthou, G. and

632 Achterberg, E. P.: Aluminium in the North Atlantic Ocean and the Labrador Sea (GEOTRACES GA01  
633 section): roles of continental inputs and biogenic particle removal, *Biogeosciences*, 15(16), 5271–  
634 5286, doi:<https://doi.org/10.5194/bg-15-5271-2018>, 2018a.

635 Menzel Barraqueta, J.-L., Klar, J. K., Gledhill, M., Schlosser, C., Shelley, R., Planquette, H., Wenzel, B.,  
636 Sarthou, G. and Achterberg, E. P.: Atmospheric aerosol deposition fluxes over the Atlantic Ocean:  
637 A GEOTRACES case study, *Biogeosciences Discuss.*, 1–25, doi:<https://doi.org/10.5194/bg-2018-209>, 2018b.

639 Mercier, H., Lherminier, P., Sarafanov, A., Gaillard, F., Daniault, N., Desbruyères, D., Falina, A., Ferron,  
640 B., Gourcuff, C., Huck, T. and Thierry, V.: Variability of the Meridional Overturning Circulation at  
641 the Greenland-Portugal Ovide section from 1993 to 2010, *Prog. Oceanogr.*, 132, 250–261,  
642 <http://dx.doi.org/10.1016/j.pocean.2013.11.001>, 2015.

643 Montero-Serrano, J. C., Frank, N., Tisnérat-Laborde, N., Colin, C., Wu, C. C., Lin, K., Shen, C. C., Copard,  
644 K., Orejas, C., Gori, A., De Mol, L., Van Rooij, D., Reverdin, G. and Douville, E.: Decadal changes in  
645 the mid-depth water mass dynamic of the Northeastern Atlantic margin (Bay of Biscay), *Earth  
646 Planet Sci Lett*, 364, 134–144, 2013.

647 Moran, S. B., Shen, C.-C., Edmonds, H. N., Weinstein, S. E., Smith, J. N. and Edwards, R. L.: Dissolved  
648 and particulate  $^{231}\text{Pa}$  and  $^{230}\text{Th}$  in the Atlantic Ocean: constraints on intermediate/deep water  
649 age, boundary scavenging, and  $^{231}\text{Pa}/^{230}\text{Th}$  fractionation, *Earth Planet Sci Lett*, 203(3–4), 999  
650 1014, doi:10.1016/S0012-821X(02)00928–7, 2002.

651 Negre, C., Zahn, R., Thomas, A. L., Masque, P., Henderson, G. M., Martinez-Mendez, G., Hall, I. R. and  
652 Mas, J. L.: Reversed flow of Atlantic deep water during the Last Glacial Maximum, *Nature*, 468,  
653 84–88, 2010.

654 Pérez, F. F., Mercier, H., Vázquez-Rodríguez, M., Lherminier, P., Velo, A., Pardo, P. C., Rosón, G. and  
655 Ríos, A. F.: Atlantic Ocean CO<sub>2</sub> uptake reduced by weakening of the meridional overturning  
656 circulation, *Nat. Biogeoscience*, doi: 10.1038/NGEO1680, 2013.

657 Pérez, F. F., Fontela, M., García-Ibáñez, M. I., Mercier, H., Velo, A., Lherminier, P., Zunino, P., Paz, M.  
658 de la, Alonso-Pérez, F., Guallart, E. F. and Padin, X. A.: Meridional overturning circulation conveys  
659 fast acidification to the deep Atlantic Ocean, *Nature*, 554(7693), 515–518,  
660 doi:10.1038/nature25493, 2018.

661 Pollard, R., Sanders, R., Lucasa, M. and Statham, P.: The Crozet Natural Iron Bloom and Export  
662 Experiment (CROZEX), *Deep Sea Res II*, 54(18–20), 1905–1914, 2007.

663 Reverdin, G., Cayan, D., Dooley, H. D., Ellett, D. J., Levitus, S., Du Penhoat, Y. and Dessier, A.: Surface  
664 salinity of the North Atlantic: Can we reconstruct its fluctuations over the last one hundred years?,  
665 *Progr Ocean.*, 33, 303–346, 1994.

666 Roca-Martí, M., Puigcorbó, V., Loeff, M. M. R. van der, Katlein, C., Fernández-Méndez, M., Peeken, I.  
667 and Masqué, P.: Carbon export fluxes and export efficiency in the central Arctic during the record  
668 sea-ice minimum in 2012: a joint  $^{234}\text{Th}/^{238}\text{U}$  and  $^{210}\text{Po}/^{210}\text{Pb}$  study, *J. Geophys. Res. Oceans*,  
669 121(7), 5030–5049, doi:10.1002/2016JC011816, 2016.

670 Sabine, C. L., Feely, R. A., Gruber, N., Key, R. M., Lee, K., Bullister, J. L., Wanninkhof, R., Wong, C. S.,  
671 Wallace, D. W. R., Tilbrook, B., Millero, F. J., Peng, T.-H., Kozyr, A., Ono, T. and Ríos, A. F.: The  
672 oceanic sink for anthropogenic CO<sub>2</sub>, *Science*, 682(305), 367–371, 2004.

673 Savidge, G., Boyd, P., Pomroy, A., Harbour, D. and Joint, I.: Phytoplankton production and biomass  
674 estimates in the Northeast Atlantic Ocean, May-June 1990, *Deep Sea Res I*, 42(5), 599–617, 1995.

675 Schlitzer, R.: Ocean Data View, online: <https://odv.awi.de>, [24 Nov 2017], 2017.

676 Seager, R., Battisti, D. S., Yin, J., Gordon, N., Naik, N., Clement, A. C. and Cane, M. A.: Is the Gulf Stream  
677 responsible for Europe’s mild winters?, *Q J R Meteorol Soc*, 128(586), 2563–2586, 2002.

678 Shelley, R. U., Roca-Martí, M., Castrillejo, M., Sanial, V., Masqué, P., Landing, W. M., van Beek, P.,  
679 Planquette, H. and Sarthou, G.: Quantification of trace element atmospheric deposition fluxes to  
680 the Atlantic Ocean (>40°N; GEOVIDE, GEOTRACES GA01) during spring 2014, *Deep Sea Res. Part  
681 Oceanogr. Res. Pap.*, 119, 34–49, doi:10.1016/j.dsr.2016.11.010, 2017.

682 Shelley, R. U., Landing, W. M., Ussher, S. J., Planquette, H. and Sarthou, G.: Regional trends in the  
683 fractional solubility of Fe and other metals from North Atlantic aerosols (GEOTRACES cruises GA01

684 and GA03) following a two-stage leach, *Biogeosciences*, 15(8), 2271–2288, doi:10.5194/bg-15-  
685 2271-2018, 2018.

686 Sutton, J. N., Souza, G. F. de, García-Ibáñez, M. I. and Rocha, C. L. D. L.: The silicon stable isotope  
687 distribution along the GEOVIDE section (GEOTRACES GA-01) of the North Atlantic Ocean,  
688 *Biogeosciences*, 15(18), 5663–5676, doi:https://doi.org/10.5194/bg-15-5663-2018, 2018.

689 Tang, Y., Castrillejo, M., Roca-Martí, M., Masqué, P., Lemaitre, N. and Stewart, G.: Distributions of total  
690 and size-fractionated particulate  $^{210}\text{Po}$  and  $^{210}\text{Pb}$  activities along the North Atlantic GEOTRACES  
691 GA01 transect: GEOVIDE cruise, *Biogeosciences*, 15(17), 5437–5453,  
692 doi:https://doi.org/10.5194/bg-15-5437-2018, 2018.

693 Tonnard, M., Planquette, H., Bowie, A. R., van der Merwe, P., Gallinari, M., Desprez de Gésincourt, F.,  
694 Germain, Y., Gourain, A., Benetti, M., Reverdin, G., Tréguer, P., Boutorh, J., Cheize, M., Menzel  
695 Barraqueta, J.-L., Pereira-Contreira, L., Shelley, R., Lherminier, P. and Sarthou, G.: Dissolved iron  
696 in the North Atlantic Ocean and Labrador Sea along the GEOVIDE section (GEOTRACES section  
697 GA01), *Biogeosciences Discuss*, 1–53, doi:10.5194/bg-2018-147, 2018.

698 Wischmeyer, A. G., Del Amo, Y., Brzezinski, M. and Wolf-Gladrow, D. A.: Theoretical constraints on the  
699 uptake of silicic acid species by marine diatoms, *Mar Chem*, 82(1–2), 13–29, 2003.

700 Xu, X., Hulbert, H. E., Schmitz Jr., W. J., Zantopp, R., Fischer, J. and Hogan, J.: On the currents and  
701 transports connected with the Atlantic Meridional Overturning Circulation in the subpolar North  
702 Atlantic, *J Geophys Res*, in press, doi: 10.1002/jgrc.20065, 2013.

703 Zunino, P., Lherminier, P., Mercier, H., Padín, X.A., Ríos, A.F. and Pérez, F.F.: Dissolved inorganic carbon  
704 budgets in the eastern subpolar North Atlantic in the 2000s from in situ data, *Geophys. Res. Lett.*,  
705 42(22), 9853–9861, doi:10.1002/2015GL066243, 2015.

706 Zunino, P., Lherminier, P., Mercier, H., Daniault, N., García-Ibáñez, M. I. and Pérez, F. F.: The GEOVIDE  
707 cruise in May–June 2014 reveals an intense Meridional Overturning Circulation over a cold and  
708 fresh subpolar North Atlantic, *Biogeosciences*, 14(23), 5323–5342, doi:10.5194/bg-14-5323-2017,  
709 2017.

710 Zurbrick, C. M., Boyle, E. A., Kayser, R. J., Reuer, M. K., Wu, J., Planquette, H., Shelley, R., Boutorh, J.,  
711 Cheize, M., Contreira, L., Menzel Barraqueta, J.-L., Lacan, F. and Sarthou, G.: Dissolved Pb and Pb  
712 isotopes in the North Atlantic from the GEOVIDE transect (GEOTRACES GA-01) and their decadal  
713 evolution, *Biogeosciences*, 15(16), 4995–5014, doi:https://doi.org/10.5194/bg-15-4995-2018,  
714 2018.

715

716 **Figure captions**

717 **Figure 1:** Schematic diagram of the mean large-scale circulation adapted from Danialt et al.  
718 (Danialt et al., 2016) and Zunino et al. (Zunino et al., 2017). Bathymetry is plotted in color  
719 with color changes at 100 and 1000m and every 1000m below 1000 m. Black dots represent  
720 the Short station, yellow stars the Large ones, orange stars the XLarge ones, and red stars the  
721 Super ones. The main water masses are indicated: Denmark Strait Overflow Water (DSOW),  
722 Iceland–Scotland Overflow Water (ISOW), Labrador Sea Water (LSW), Mediterranean Water  
723 (MW), and lower Northeast Atlantic Deep Water (LNEADW).

724 **Figure 2:** Section plots for (a) salinity, (b) potential temperature ( $^{\circ}\text{C}$ ), (c) dissolved oxygen  
725 ( $\mu\text{mol kg}^{-1}$ ), (d) nitrate + nitrite ( $\mu\text{mol L}^{-1}$ ), and (e) silicic acid ( $\mu\text{mol L}^{-1}$ ) during the GEOVIDE  
726 cruise. Water masses are indicated in black, MW: Mediterranean Water; ENACW: North  
727 Atlantic Central Water; NEADW: North East Atlantic Deep Water; LSW: Labrador Sea Water;  
728 ISOW: Iceland-Scotland Overflow Water; SAIW: Sub-Arctic Intermediate Water; IcSPMW:  
729 Iceland Sub-Polar Mode Water; IrSPMW: Irminger Sub-Polar Mode Water. Station locations  
730 are indicated by the numbers on top of the panel. These plots were generated by Ocean Data  
731 View (Schlitzer, 2017).

732 **Figure 3:** Section plots for (a) biogenic silica (BSi,  $\mu\text{mol L}^{-1}$ ), (b) particulate organic carbon (POC,  
733  $\mu\text{mol L}^{-1}$ ), and (c) particulate organic nitrogen (PON,  $\mu\text{mol L}^{-1}$ ), during the GEOVIDE cruise.  
734 Station locations are indicated by the numbers on top of the panel. These plots were  
735 generated by Ocean Data View (Schlitzer, 2017).

736

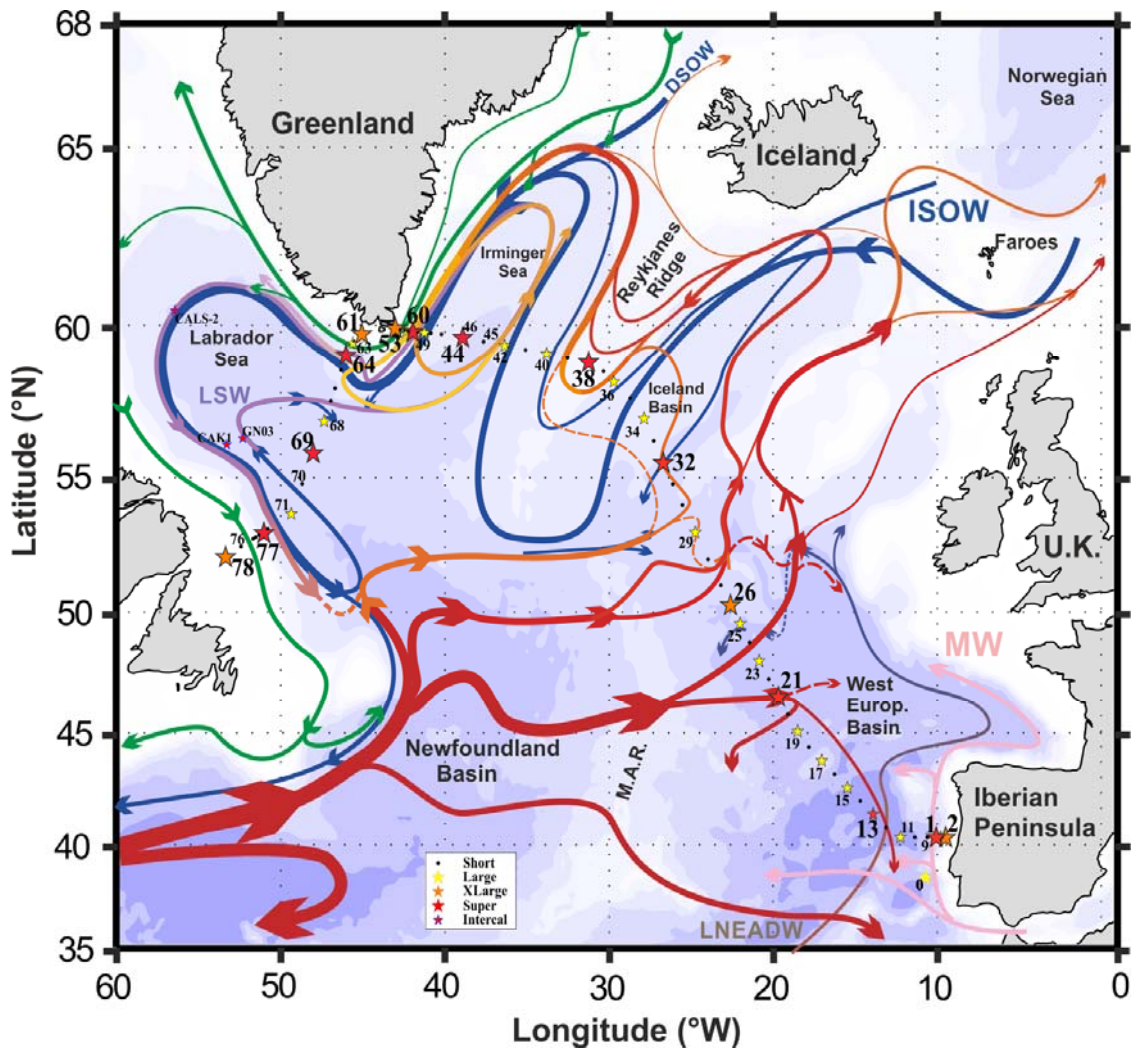
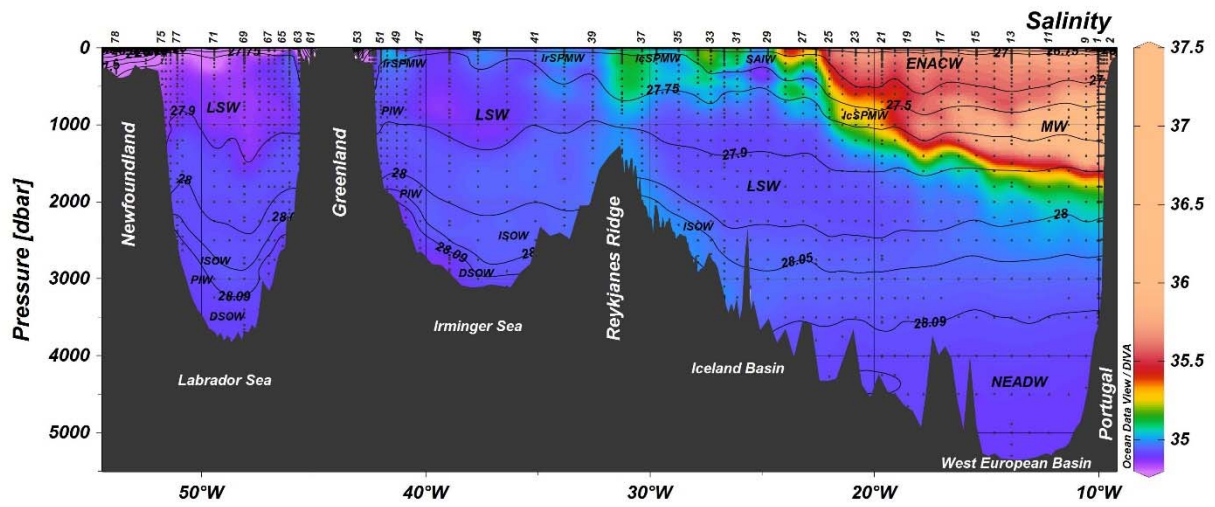
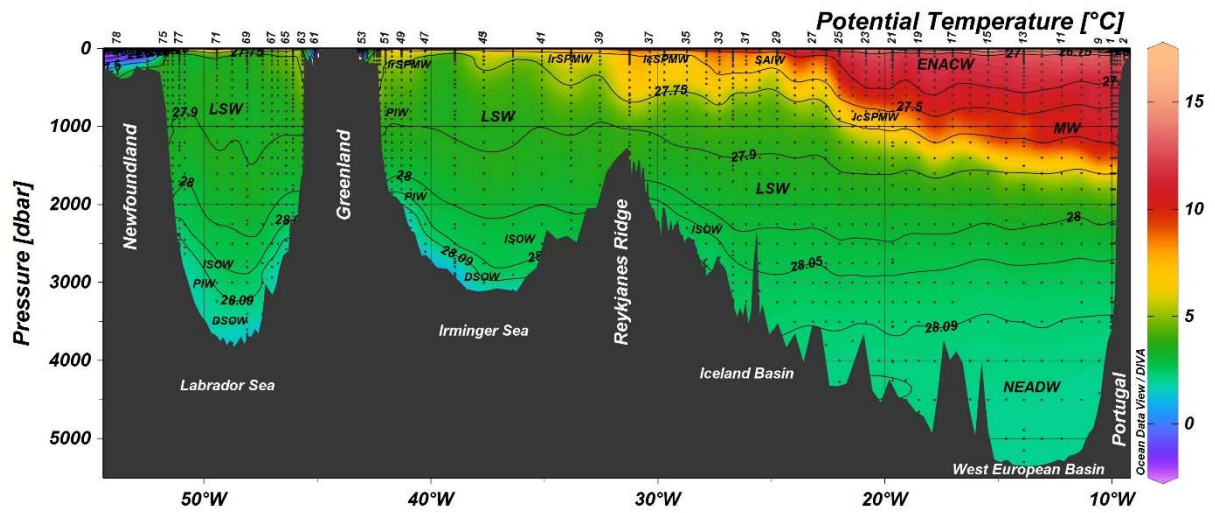


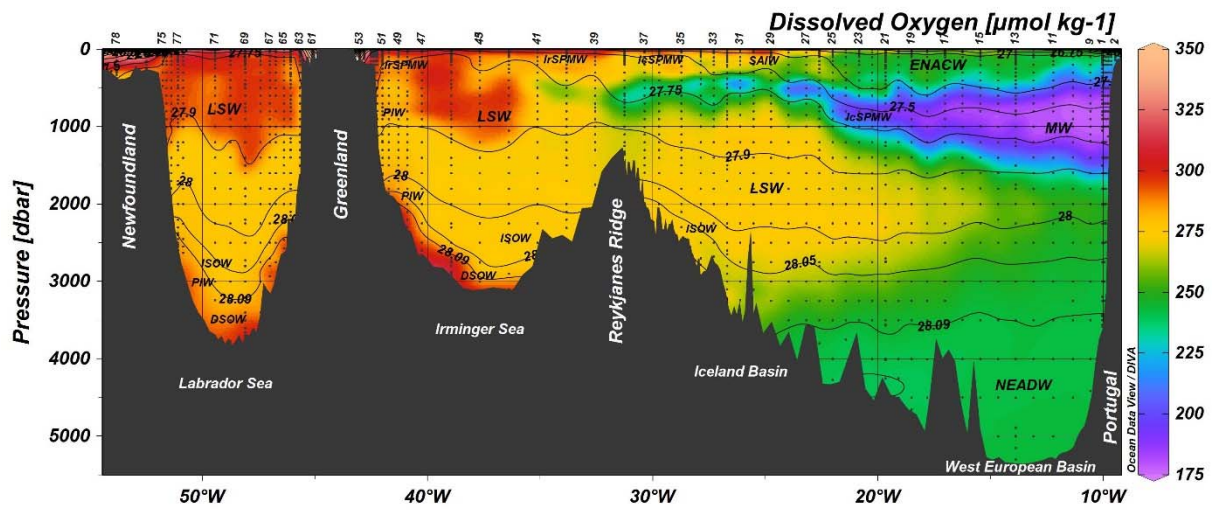
Figure 1



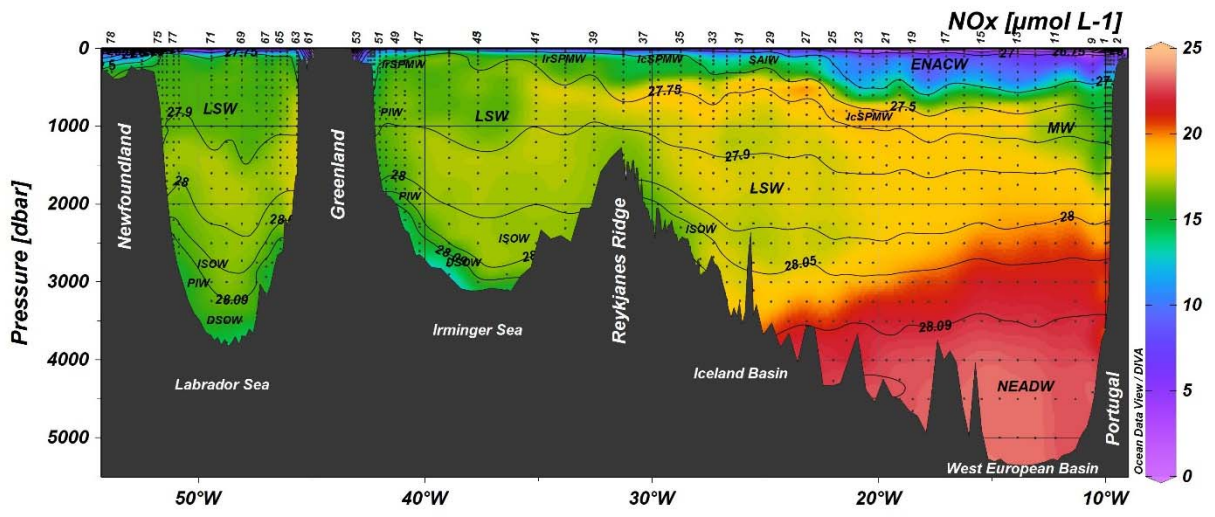
(a)



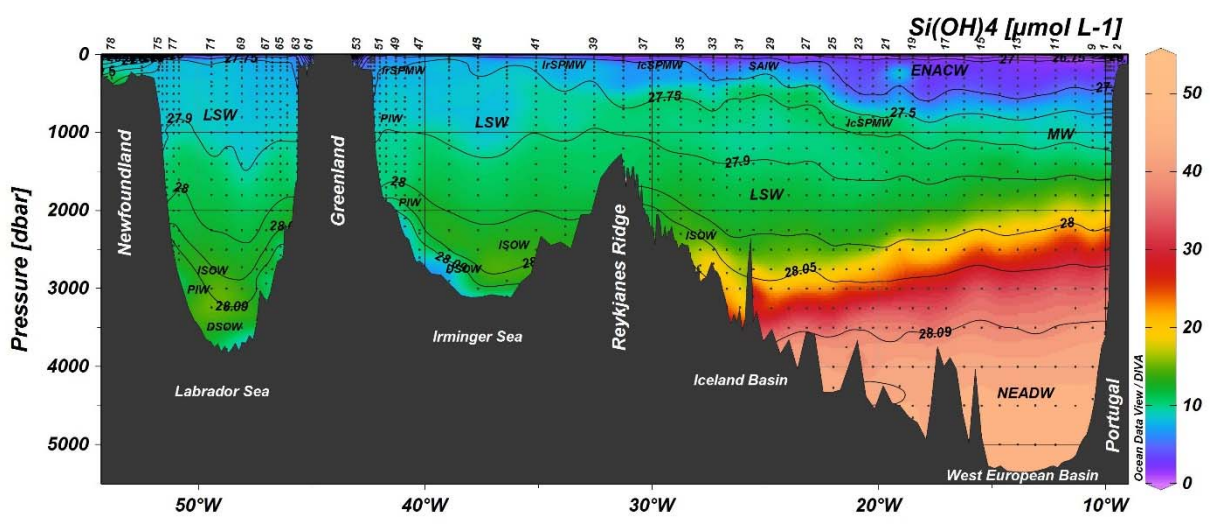
(b)



(c)

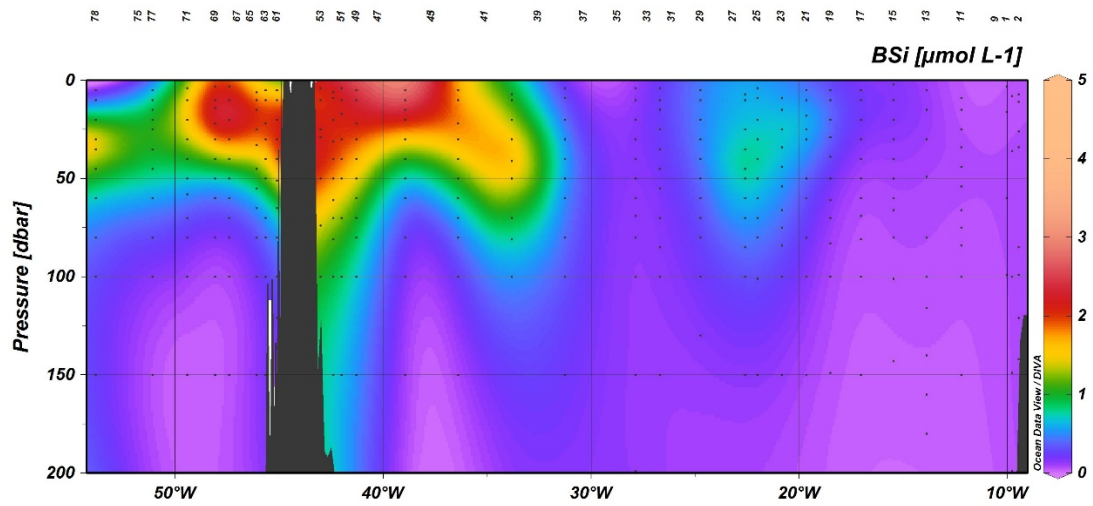


(d)

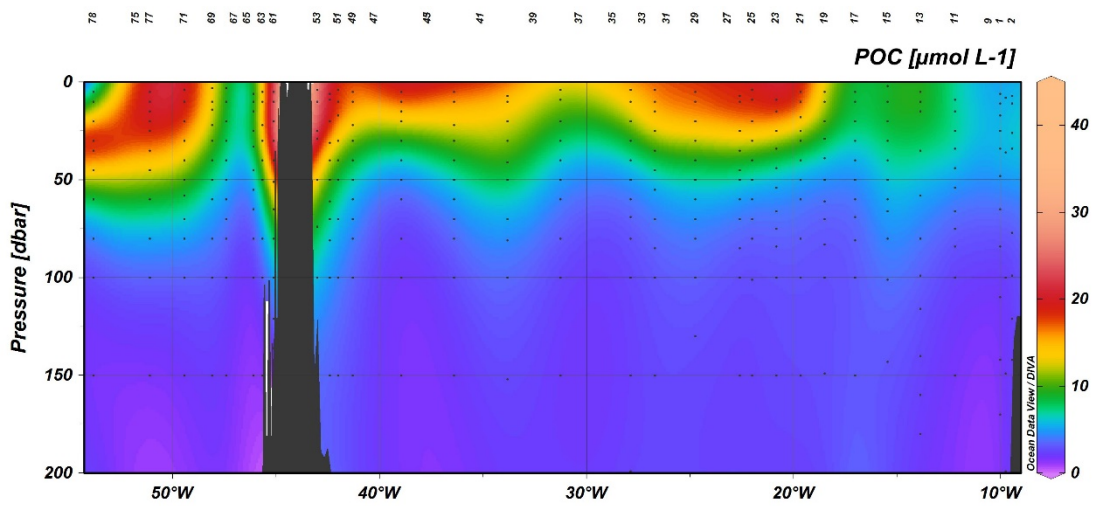


(e)

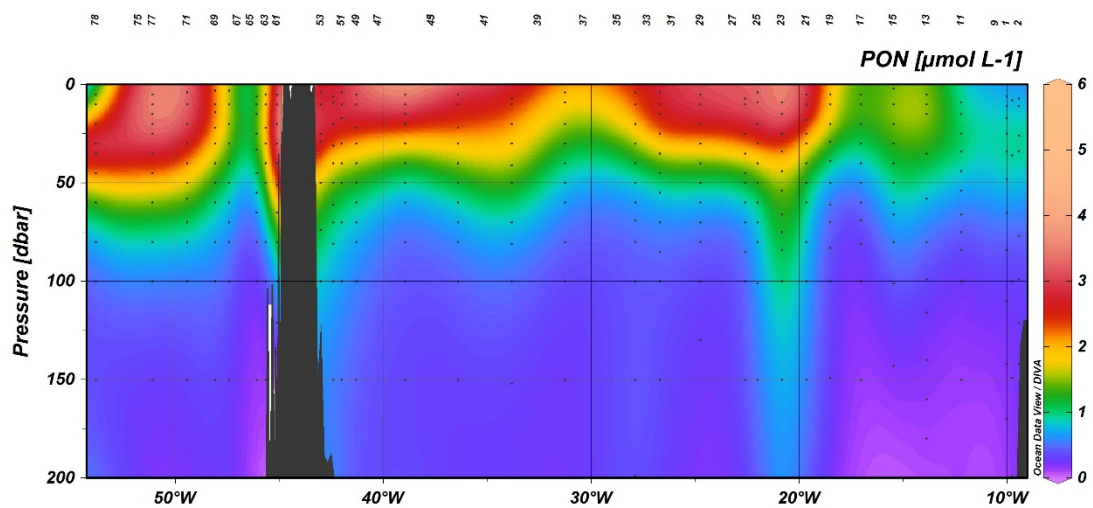
Figure 2



(a)



(b)



(c)

Figure 3